Three-Dimensional Elastic Compatibility and Varieties of Twins in Martensites

K. Ø. Rasmussen,[1] T. Lookman,[1] A. Saxena,[1] A. R. Bishop,[1] R. C. Albers,[1] and S. R. Shenoy[2]

[1]*Theoretical Division, Los Alamos National Laboratory, Los Alamos, New Mexico 87545*

[2]*Abdus Salam International Centre for Theoretical Physics, Trieste 34100, Italy*

(Received 28 January 2000; published 16 July 2001)

We model a cubic-to-tetragonal martensitic transition by a Ginzburg-Landau free energy in the symmetric strain tensor. We show in three dimensions (3D) that solving the St. Venant compatibility relations for strain, treated as independent field equations, generates three anisotropic long-range potentials between the two order parameter components. These potentials encode 3D discrete symmetries, express the energetics of lattice integrity, and determine 3D textures. Simulation predictions include twins with temperature-varying orientation, helical twins, competing metastable states, and compatibility-induced elastic frustration. Our approach also applies to improper ferroelastics.

DOI: 10.1103/PhysRevLett.87.055704 PACS numbers: 64.70.Kb, 61.72.Cc, 81.30.Kf, 82.65.+r

Strain plays a crucial role in many structural phase transitions, either as a primary order parameter (OP), e.g., in martensites [1] and shape-memory alloys [2], or as a secondary OP, e.g., in ferroelectric [3] and magnetoelastic [4] materials. Complex, nonuniform, and temperature-dependent strain variations or elastic textures, e.g., a rich variety of twins, form spontaneously, as seen by high resolution electron microscopy (HREM) and neutron scattering studies. In alloys such as Ni_xAl_{1-x}, martensite forms with a long period stacking structure involving (110) planes [5], while in Fe_xPd_{1-x}, (011) twins preferentially grow at the expense of (101) twins as the temperature is lowered [6]. Intrinsically inhomogeneous states of spin and charge in high-temperature superconductors [7] and colossal magnetoresistance manganites [8] are the subject of intense study and could be understood as induced by coupling to the strain tensor [9]. Thus a deeper understanding of complex 3D twins in martensites through a Ginzburg-Landau (GL) description in terms of the OP strain tensor components alone may be more widely relevant.

Displacive martensites have been modeled through a GL free energy F that is anharmonic ("triple-well") in the OP strain tensor components and harmonic in the non-OP components. However, in both analytic and simulation work, the *displacement* $\vec{u}(r)$ has conventionally been chosen [10–12] as the independent variable. The physical requirement of smoothly fitting deformed unit cells, without defects such as dislocations or vacancies, is enforced through demanding the single valuedness of $\vec{u}$. The strain tensor appearing in F is merely a symbol for gradients of $\vec{u}$. Analogously, in electromagnetism the vector potential $\vec{A}$ can be the independent variable, and the absence of magnetic monopoles can be enforced by requiring its single valuedness, with the magnetic field as a derived quantity. However, we know that an alternative treatment of electromagnetism regards the physical magnetic field $\vec{B}$ as the only independent variable and takes $\vec{\nabla} \cdot \vec{B} = 0$ as a "no-monopole" independent dynamical field equation. Similarly, elasticity can also be usefully treated in terms of only the physical *strain tensor* $\epsilon_{ij}(r)$. The St. Venant's compatibility condition $\nabla \times (\nabla \times \epsilon)^{\dagger} = 0$ [13], which is merely an incidental identity when expressed in terms of $\vec{u}$, can be elevated to the status of "no-defect" independent dynamical field equation [14]. For the 2D square-to-rectangle transition, solving this differential equation linking strain tensor components allows non-OP strains in the free energy to be written in terms of the single deviatoric OP strain alone. This yields one texture-inducing, anisotropic long-range (ALR) potential between OP strains in the bulk. To show this strain-only approach works more generally, we must consider realistic 3D lattices of richer discrete symmetries, and multicomponent OP strains.

In this Letter we show for the first time, using the example of the cubic-to-tetragonal transition, that an OP strain-only compatibility-based description of 3D martensites is possible. We obtain a GL understanding of textures in terms of the two OP strain components, with three bulk ALR forces that encode the discrete cubic unit-cell symmetry, express the energetics of 3D lattice integrity, and determine 3D textures. In simulations we find twins with a temperature-dependent orientation, twins with an interplane helical twist, and frustrationlike competition between free energy minima. These features have no 2D analog, and some are similar to experiment. Others are predictions for high resolution microscopies.

The procedure, which can be carried out also for proper ferroelastic transitions of *all seven crystal systems,* is as follows. The GL free energy contains both anharmonic terms in the (two) OP deviatoric strains and harmonic terms in the "non-OP" compressional and (three) shear strains. A constrained minimization in terms of the non-OP strains incorporating six St. Venant compatibility equations yields the desired effective free energy F in terms of the OP strains alone. The OP textures that minimize this F automatically satisfy elastic compatibility, and non-OP textures are derived from them. We note that for real, finite systems, there are *two* types of ALR compatibility forces: bulk and surface. The latter arise from the boundary conditions at surfaces such as habit planes (i.e., austenite-martensite or parent-product boundaries) and can impose

a system-size dependent twin width [10,14]. However, for simplicity, we focus here only on the bulk compatibility potential and periodic boundary conditions.

Model.—For the cubic-to-tetragonal transition, the symmetry-adapted strains e_i can be defined in terms of the Lagrangian strain tensor components ϵ_{ij} as the dilatation $e_1 = (1/\sqrt{3})(\epsilon_{11} + \epsilon_{22} + \epsilon_{33})$, the two deviatoric (i.e., OP) strains $e_2 = (1/\sqrt{2})(\epsilon_{11} - \epsilon_{22})$, $e_3 = (1/\sqrt{6})(\epsilon_{11} + \epsilon_{22} - 2\epsilon_{33})$, and the three shear strains $e_4 = 2\epsilon_{23}$, $e_5 = 2\epsilon_{13}$, $e_6 = 2\epsilon_{12}$. The elastic energy in 3D is given by [15] $F = F_L(e_2, e_3) + F_{\text{grad}}(\nabla e_2, \nabla e_3) + F_{cs}(e_1, e_4, e_5, e_6)$, where the Landau free energy (Fig. 1) summed over unit cells, is

$$F_L = \sum\nolimits_r A(e_2^2 + e_3^2) + Be_3(e_3^2 - 3e_2^2) + C(e_2^2 + e_3^2)^2.$$

The Ginzburg (or gradient) contribution, which is responsible for the interfacial energies, ignoring non-OP gradients as of secondary importance, is

$$\begin{aligned} F_{\text{grad}} = \sum\nolimits_r g\Big[& (e_{2,x}^2 + e_{2,y}^2) + \frac{1}{3}(e_{3,x}^2 + e_{3,y}^2) \\ & + \frac{2}{\sqrt{3}}(e_{2,x}e_{3,x} - e_{2,y}e_{3,y}) + \frac{4}{3}e_{3,z}^2\Big] \\ + \sum\nolimits_r h\Big[& (e_{3,x}^2 + e_{3,y}^2) + \frac{1}{3}(e_{2,x}^2 + e_{2,y}^2) \\ & - \frac{2}{\sqrt{3}}(e_{2,x}e_{3,x} - e_{2,y}e_{3,y}) + \frac{4}{3}e_{2,z}^2\Big], \end{aligned}$$

where the x, y, z subscripts refer to corresponding derivatives. The harmonic elastic energy contribution due to non-OP compression/shear (CS) strain components is

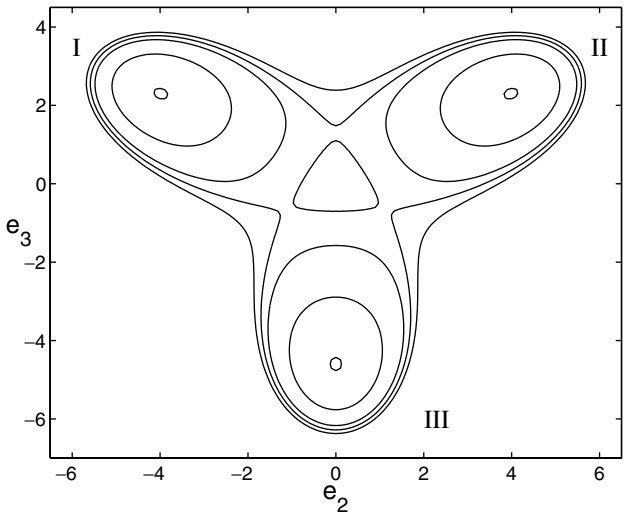

FIG. 1. Contour plot of the Landau free energy in the martensite phase depicting the three degenerate energy minima corresponding to the three tetragonal variants with tetragonal axis along the x, the y, and the z axis, respectively. Parameters are $A = -1.0$, $B = 0.83$, and $C = 0.04$.

$$F_{cs} = \sum\nolimits_r A_c e_1^2 + A_s(e_4^2 + e_5^2 + e_6^2)$$

and is *symmetry distinguished* from harmonic parts of the OP free energy F_L. We do not consider a coupling, $F_{\text{compos}}(\eta, \nabla\eta, e_2, e_3)$, of the OP strain to compositional fluctuations η, which is responsible for tweed.

The coefficients $A = A_o(T - T_o)$, B, and C are related to the second, third, and fourth order elastic constants, respectively, and are obtainable from experimental structural data. A_c and A_s are the (bulk) compression and shear moduli, respectively. The parameter T_o is the martensitic transition temperature and the gradient coefficients g and h can be determined from the phonon dispersion near the Brillouin zone center or from a direct HREM observation of the twin boundary width.

3D compatibility and analysis.—The six compatibility conditions on the strain components are the cyclic permutations in tensor labels 1, 2, 3 of the two equations: $C^{(1)} = \epsilon_{23,yz} - \epsilon_{22,zz} - \epsilon_{33,yy} = 0$ and $C^{(2)} = 2\epsilon_{11,yz} + \epsilon_{23,xx} - \epsilon_{31,xy} - \epsilon_{12,xz} = 0$. The six equations can all be recast in terms of the symmetry-adapted $e_i(r)$ strains, which transform irreducibly under the space group $Pm\bar{3}m$. The compatibility constraints can be enforced in F through six Lagrange multipliers $\Lambda^{(\ell)}(\vec{r})$, with $\ell = 1, 2, \ldots, 6$: $\delta[F_{cs}(e_1, e_4, e_5, e_6) + \sum_\ell \sum_r \Lambda^{(\ell)} C^{(\ell)}] = 0$.

Since F_{cs} is harmonic in the four non-OP strain fields, their independent variations allow them to be written in terms of derivatives of the six Lagrange multipliers (and, of course, the OP fields). Substituting back into the six compatibility equations and using Fourier transforms permits an elimination of $\Lambda^{(\ell)}$ and finally yields e_1, e_4, e_5, e_6 in terms of the OP e_α with $\alpha = 2, 3$.

The bulk compression/shear term can be written as

$$F_{cs}^{\text{bulk}} = \sum\nolimits_{\alpha,\alpha'} \sum\nolimits_k e_\alpha(\vec{k}) U_{\alpha\alpha'}(\vec{k}) e_{\alpha'}^*(\vec{k}).$$

The bulk kernels U_{22}, U_{23}, and U_{33} in Fourier space, which we display in contour plots (Fig. 2) but do not explicitly write out, are complicated functions of $\vec{k}$ that are clearly strongly anisotropic. At long wavelengths they depend only on ratios of components k_x, k_y, and k_z, so in spherical polar coordinates, $U_{\alpha\alpha'}(\vec{k}) = U_{\alpha\alpha'}(\theta, \phi)$. They vary with wave vector direction angles θ and ϕ but are independent of magnitude $|\vec{k}|$ and so do not set a mesoscopic length scale. In coordinate space, $F_{cs}^{\text{bulk}} = \sum\sum e_\alpha(\vec{r}) U_{\alpha\alpha'}(\vec{r} - \vec{r}') e_{\alpha'}(r')$, with the ALR kernels $U(R) \sim 1/R^d$, where $d = 3$ comes from phase space. The anisotropies of the three kernels encode the full discrete symmetries of the 3D cubic-to-tetragonal transformation: F_{cs}^{bulk} is invariant under the operations of the point group $m\bar{3}m$. The corresponding 2D case shows [14] important differences.

First, in 3D there are three kernels in F_{cs}^{bulk} with different favored directionalities: competing nonzero energy minima can produce *orientational elastic frustration*. Second, F_{grad} in Fourier space depends on *both* $|\vec{k}|$ and θ, ϕ so the lowest-energy orientation from the combination

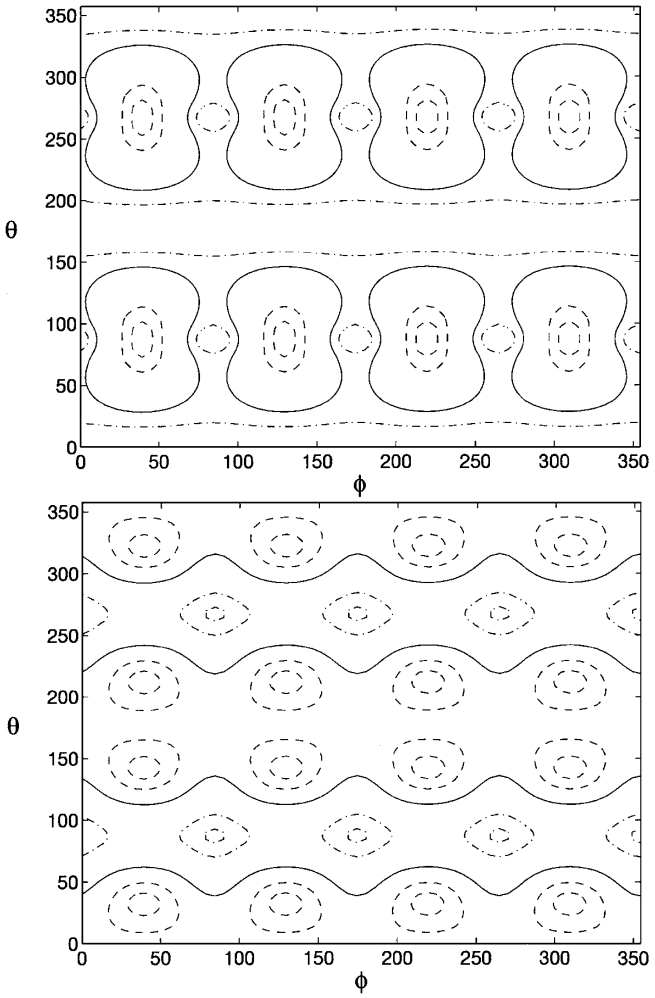

FIG. 2. 3D compatibility kernels U_{22} (upper) and U_{33} (lower) as a function of the colatitude θ and the azimuth ϕ angles. Dashed contours surround minima, and dash-dotted contours surround maxima, while solid contours show intermediate levels. $A_s = 1.2$ and $A_c = 2.4$. U_{23} is not shown.

$F_{cs}^{\text{bulk}} + F_{\text{grad}}$ is at a *nonzero* $|\vec{k}|$: there is an *internal textural length*. Third, the combination involves *weighted* sums, with OP field e_2, e_3 acting as weights. Since the e_2, e_3 relative magnitudes are temperature dependent as determined by F_L, this change of weights can yield *temperature-varying orientations* within the martensite phase.

In 2D, by contrast, with one OP, an *isotropic* gradient term dependent only on $|\vec{k}|$, and one bulk orienting potential [11,14], there is only one directional zero-energy minimum that is *independent* of the amplitude of the strain field. Hence there is no elastic frustration or internal twin scale. A size-dependent twin width [10] is induced by the surface contribution F_{cs}^{surface} [14].

Figure 2 shows contours of kernels U_{22} and U_{33} as functions of the angles θ and ϕ. The minima define a direction in 3D in which the compression-shear energy arising from the particular kernel is minimal. There exist multiple minima, i.e., microstructures of differing orientation.

Texture simulations.—The various energy-minimizing martensitic textures are found from random initial conditions and relaxational dynamics for the *OP strains*. That is, $\dot{e}_\alpha(r) = -\delta F(e_2, e_3)/\delta e_\alpha(r)$, with $\alpha = 2, 3$ and the time t is scaled with a characteristic relaxation rate. The system is a regular 32^3 cube with periodic boundary conditions. To ensure fully equilibrated textures in $e_2(r)$ and $e_3(r)$, we monitor the energy flattening with time over long runs of 10^5 time steps ($\Delta t = 10^{-3}$), and the robustness of textures to noise.

We illustrate the simulation results obtained with representative (scaled) parameters. The red/blue/green colors represent (e_2, e_3) positive/negative/zero OP strain values, respectively (the actual values are approximately determined by the minima of F_L, as illustrated in Fig. 1).

Figure 3 shows the simplest twinning texture [(110) twins] that is uniform in the z direction. The strain e_2 changes from negative (minimum I in Fig. 1) to positive (minimum II in Fig. 1) (i.e., blue to red). The strain e_3 is not shown, as it is essentially constant with a small modulation at the twin boundaries. This particular martensitic texture is the trivial extension of the (diagonally oriented) 2D results [14] since the OP fields are uniform in the z direction.

A richer texture is shown in Fig. 4, where the strain e_3 changes from negative (minimum III in Fig. 1) to positive (minimum I or II in Fig. 1), i.e., blue to red. The strain e_2 would be either zero (green) when e_3 is negative (minimum III) or positive/negative when e_3 is positive. The figure clearly shows helical twins with strain e_2 that can be oriented in two possible ways, reflecting the inversion symmetry of the kernels with respect to x, y. We note that a similar alternating stripe-direction microstructure has been implied by neutron and x-ray scattering studies in layered high-temperature superconductors [7].

To illustrate the effect of frustration that is inherent in the compatibility relations, we explain the orientation of the twins (Fig. 4). We evaluate free energy for the red

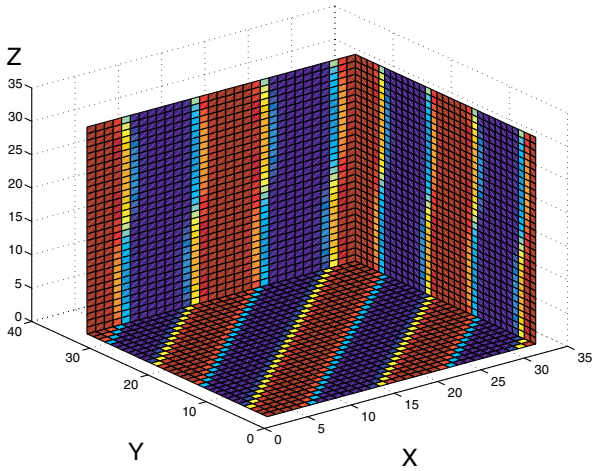

FIG. 3 (color). 3D twins in the (110) plane obtained from the time-dependent GL simulations, with representative parameters as given in Figs. 1 and 2, and $h = 1$ and $g = 1$. The twin scale is determined by the competition between the Ginzburg energy and the bulk compression/shear energy.

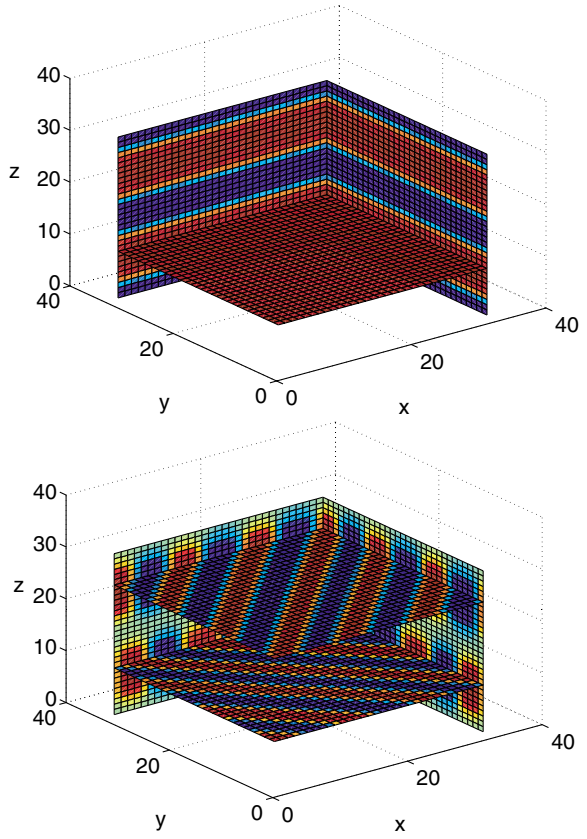

FIG. 4 (color). 3D twins with two different orientations, (110) and $(1\bar{1}0)$, in adjacent planes. Both OP fields are shown, e_3 in the upper panel and e_2 in the lower panel.

and blue twins, respectively, using the appropriate values of the strains e_2 and e_3 in the twins. Figure 5 depicts this energy in the θ-ϕ plane. The dashed (solid) line shows the minimum corresponding to the blue (red) twins. We note that the minima correspond to different ϕ angles ($45 + \delta$ and $45 - \delta$). The shift δ depends on the parameters of the Landau free energy. The red and blue twins have different and conflicting optimal orientations, accommodated by both choosing the average angle of 45°. This aspect of competing metastable states is a novel feature associated with the cubic symmetry kernels, leading to a rich landscape of predicted microstructures.

Conclusion.—We have derived a complete symmetry based, strain-only, fully 3D model that describes texturings around the cubic-to-tetragonal structural transitions that occur in many martensitic and shape-memory alloys. We obtained analytically three compatibility-induced anisotropic long-range potentials between the two deviatoric OP strains. Many twin orientations are possible in 3D as a result of elastic frustration and the "landscape" (probably "rugged") of metastable energy states. Image reconstruction methods of data from HREM and neutron scattering will allow a more quantitative comparison of strain patterns with those predicted here. Our model can be straightforwardly generalized to improper ferroelastic transitions by including symmetry allowed polarization/magnetization nonlinear terms, and couplings to strain [9]. Other symmetries can be handled. For example, we have also studied the cubic-to-trigonal (rhombohedral) transition in lead orthovanadate and NiTi- and AuCd-based shape-memory alloys using the three shear strains e_4, e_5, and e_6 as OP and with e_1, e_2, and e_3 expressed in terms of the shear strains via compatibility. Finally, we note that for an inclusion of tetragonal symmetry ($e_2 = 0$, $e_3 = e_0$) the kernels yield a strain field $\sim e_0/r^3$, as in Eshelby's result [16].

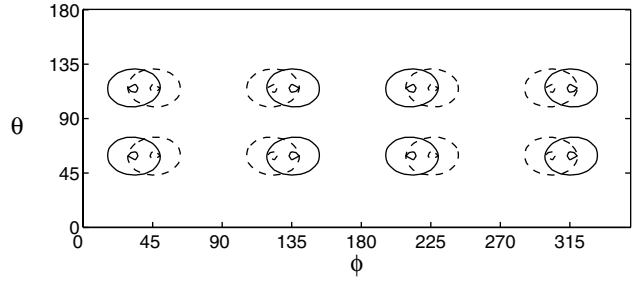

FIG. 5. Free energy of the red and blue twins illustrating inherent strain (orientational) frustration in 3D.

We thank G. R. Barsch and I. Mitkov for insightful discussions. This work was supported by the U.S. DOE (Contract No. W-7405-Eng-36).

[1] Z. Nishiyama, *Martensitic Transformations* (Academic, New York, 1978).
[2] *Shape Memory Materials,* edited by K. Otsuka and C. M. Wayman (Cambridge University Press, Cambridge, U.K., 1998).
[3] J. C. Slonczewski and H. Thomas, Phys. Rev. B **1**, 3599 (1970).
[4] R. D. James and M. Wuttig, Philos. Mag. A **77**, 1273 (1998).
[5] D. Schryvers and L. E. Tanner, Ultramicroscopy **32**, 241 (1990).
[6] M. Sugiyama Ph.D. thesis, Osaka University, 1985.
[7] T. Noda *et al.,* Science **286**, 265 (1999).
[8] T. Kimura *et al.,* Phys. Rev. B **53**, 8733 (1996).
[9] A. R. Bishop *et al.* (unpublished).
[10] G. R. Barsch *et al.,* Phys. Rev. Lett. **59**, 1251 (1987).
[11] S. Kartha *et al.,* Phys. Rev. B **52**, 803 (1995). These 2D simulations were in $\vec{u}$, with "strains" in the free energy $F(\vec{u})$ as $\vec{u}$ gradients. Observed textures were then attributed to implicit strain-strain forces. Our 3D simulations here are in the OP strain(s) only, with an $F(e_2, e_3)$ explicitly containing our calculated 3D ALR potentials.
[12] Within the phase-field model, which involves a $\vec{u}$ description, 3D simulations have been performed [Y. Wang and A. G. Khachaturyan, Acta Mater. **45**, 759 (1997)].
[13] D. S. Chandrasekharaiah and L. Debnath, *Continuum Mechanics* (Academic Press, San Diego, 1994), p. 218.
[14] S. R. Shenoy *et al.,* Phys. Rev. B **60**, R12 537 (1999).
[15] G. R. Barsch and J. A. Krumhansl, Phys. Rev. Lett. **53**, 1069 (1984); Metall. Trans. A **19**, 761 (1988).
[16] J. D. Eshelby, Solid State Phys. **3**, 79 (1957).